Parity-time symmetric waveguides coupled through chiral materials

A. De Corte,[1] M. Besbes,[2] H. Benisty,[2] and B. Maes[1]

[1] University of Mons, Micro- and Nanophotonic Materials Group, Research Institute for Materials Science and Engineering, University of Mons, 20 Place du Parc, B-7000 Mons, Belgium
[2] Laboratoire Charles Fabry, Institut d'Optique Graduate School, CNRS, Université Paris Saclay, 2 Av. Augustin Fresnel, 91127 Palaiseau Cedex, France

Parity-time (PT) symmetry can be achieved in a standard photonic structure formed by coupled waveguides with balanced gain and loss. It is characterized by a mode dispersion changing abruptly from propagating modes (PT-symmetric) to amplified/decaying modes (PT-broken), at a certain value of gain/loss called the exceptional point (EP). We investigate the impact of inserting a material with chirality in the gap between two rectangular coupled PT-symmetric waveguides. At degeneracies between TE- and TM-polarized achiral modes, we observe a variety of avoided crossings dependent on the PT nature of the interacting modes. Same-symmetry modes split into an anticrossing under the effect of chirality, whereas for opposite-symmetry modes chirality creates a PT-broken zone. Interestingly, a trimodal anticrossing arises at the EP, which reaches a chiral sensitivity of bulk media despite the narrowness of the chiral inclusion. We obtain these results using both a finite element method mode solver tuned to enable chiral material modelling, and a coupled-mode equations model that includes chiral couplings, leading to a good match between simulations and theory.

Introduction

Coupled waveguides with balanced gain and loss form a standard photonic structure for the study of parity-time (PT) symmetry and its unique associated features. In this structure, the two waveguides have opposite imaginary refractive indices, defined by the gain/loss parameter γ, which determines the operating regime: PT-symmetric when the two main waveguide modes propagate without gain or loss, and PT-broken when one mode is amplified and the other decays. The transition between these two regimes occurs at the exceptional point (EP) causing abrupt changes of the propagation constants.

Chiral structures and chiral materials, on the other hand, respond differently to left-handed and right-handed circularly polarized light. This contrast is highly desired for enantiomer detection in chemistry and biology [2] and it has been shown that PT-symmetry can enhance it in a multilayer approach [3].

In this work, we combine both approaches and insert a chiral material in the gap between the two waveguides of a PT-symmetric pair in order to study the influence of chirality on the waveguide dispersion.

Structure

Our structure is composed of two rectangular PT-symmetric waveguides, one made of a gain material, the other with loss (Fig. 1a). We employed a waveguide width of 100nm and thickness of 400nm, for a vacuum wavelength of 350nm (but the phenomena can be rescaled to other sizes and wavelengths). The gap width between the waveguides varies between 10 and 50 nm. The gain and loss materials are characterized by a refractive index of $2 - i\gamma$ and $2 + i\gamma$, respectively, γ being the gain/loss parameter.

The gap material can possess a nonzero chirality parameter κ defined via the chiral constitutive relations [3]: $\vec{D} = \varepsilon\vec{E} - i\frac{\kappa}{c}\vec{H}$ and $\vec{B} = \mu\vec{H} + i\frac{\kappa}{c}\vec{E}$ where $\vec{D}$, $\vec{E}$ are the electric displacement and field, $\vec{B}$, $\vec{H}$ are the magnetic induction and field, ε is the electric permittivity, μ is the magnetic permeability, c is the speed of light in vacuum, and i is the imaginary number. We simulate our setup using the mode solver of the SimPhotonics Matlab toolbox, a Maxwell equations' solver developed at Laboratoire Charles Fabry, upgraded to enable finite element method (FEM) modelling of chiral materials.

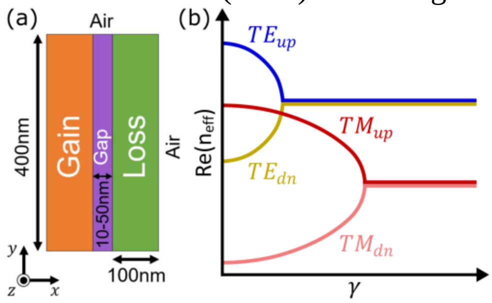

Figure 1 – (a) PT-symmetric rectangular waveguides (orange and green, non chiral) and chiral gap (purple), with mode propagation along z. The device is embedded in air. (b) Schematic of typical TE (blue and gold) and TM (red and pink) real dispersions of the structure as a function of the gain/loss parameter γ.

Chiral impact on the guided modes

In this section we assess the effect of chirality on the PT mode dispersion obtained by FEM calculations. We refer to the modes with a dominant y electric or magnetic field component as quasi-TE or quasi-TM, respectively. Due to the x-axis symmetry of the structure, a symmetric mode and an antisymmetric mode form a fork in the PT mode dispersion – as a function of the gain/loss parameter γ – for each polarization (see Fig. 1b). We employ the subscripts up and dn to refer to symmetric and antisymmetric modes, respectively. The structure is designed such that, depending on the gap width (that basically controls the $\gamma = 0$ branch splitting), the TM_{up} dispersion (red in Fig. 1b) crosses the TE-fork at a specific place: through the upper part TE_{up} (blue in Fig. 1b), through the lower part TE_{dn} (gold in Fig. 1b), or precisely at the TE EP.

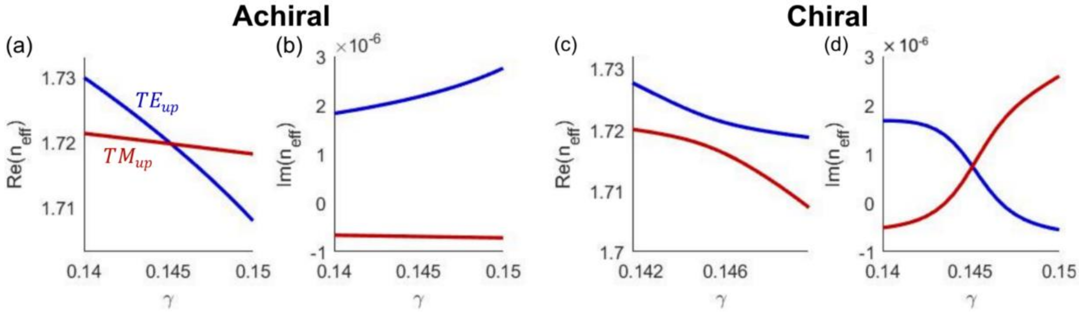

Figure 2 – Effect of chirality on the dispersion for a narrow gap: Dispersion of modes TE_{up} (blue) and TM_{up} (red) around their crossing for an (a,b) achiral and (c,d) chiral 12nm gap.

For narrow gaps, the achiral dispersion of mode TM_{up} (red in Fig. 2a,b) crosses the dispersion of mode TE_{up} (blue). Two modes having the same parity thus cross dispersions (here with symmetric profiles). In that case, chirality splits the effective indices into two values: the achiral dispersion curves (Fig. 2a) spread apart around the crossing (Fig. 2c), while remaining real, as $Im(n_{eff})$ is negligible (Fig. 2b,d). This is expected; chirality lifts the TE-TM degeneracy, much as it does in bulk chiral materials (optical activity).

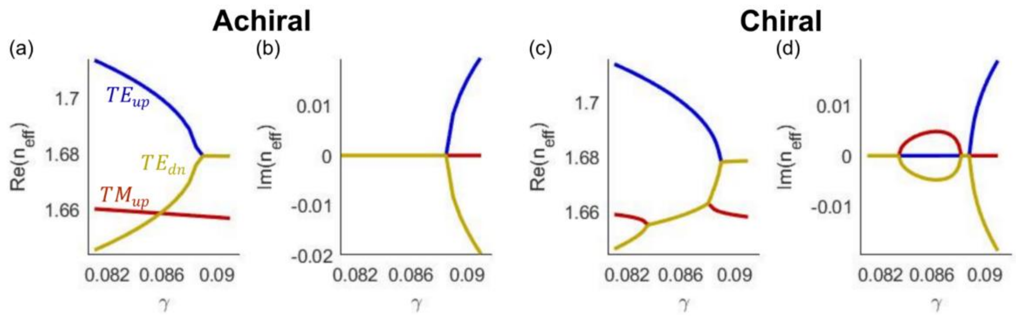

Figure 3 - Effect of chirality on the dispersion for a broad gap: Dispersion of modes TE_{up} (blue), TM_{up} (red) and TE_{dn} (gold) around the TE EP for an (a,b) achiral and (c,d) chiral 44nm gap.

For broad enough gaps, the dispersion of mode TM_{up} crosses the lower part of the TE PT fork. Two modes of different parity thus become degenerate: TM_{up} with a symmetric profile and TE_{dn} with an antisymmetric profile (red and gold in Fig. 3a,b). Intriguingly, chirality induces the appearance of a PT-broken zone in the PT-symmetric regime around the crossing (0.083-0.088 in Fig. 3c,d). The effective indices of the two modes present equal real parts (Fig. 3c) and acquire a substantial imaginary part in this range (Fig. 3d). At both ends of the locally broken 'bubble' there are thus two new exceptional points, with the second one (γ = 0.088) recovering the PT-symmetry of the dispersion. Local symmetry breaking followed by symmetry recovery has already been observed e.g. in four-waveguide systems [4], but here chirality offers the same possibility with only two waveguides by allowing quasi-TE and quasi-TM modes to couple.

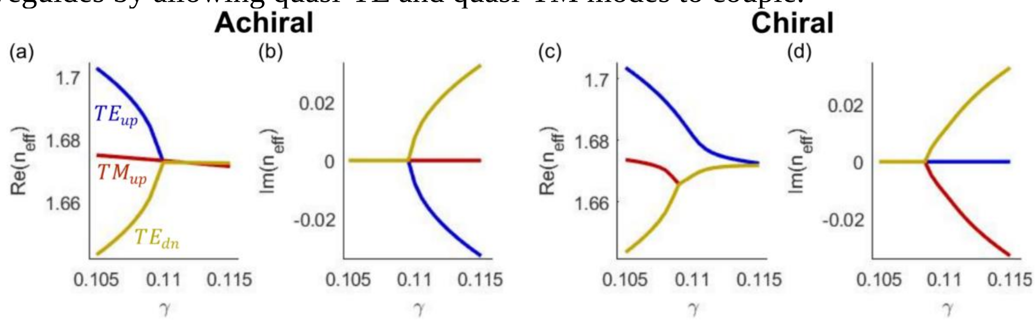

Figure 4 - Effect of chirality on the dispersion for a medium gap: Dispersion of modes TE_{up} (blue), TM_{up} (red) and TE_{dn} (gold) around the TE EP for an (a,b) achiral and (c,d) chiral 32nm gap.

For a medium gap width, the TM_{up} dispersion (red in Fig. 4a,b) crosses the TE fork exactly at the EP (zoom in Fig. 4a,b) and thus interacts with both TE modes (blue and gold), resulting in a hybrid coupling. Indeed, at the TE EP, TE_{up} and TE_{dn} modes coalesce. The blue and red curves spread apart in Fig. 4c similarly to an anticrossing, while the real dispersions of TM_{up} (red) and TE_{dn} (gold) join together in an EP. Through this process the EP is slightly shifted (Fig. 4d), and the PT-broken regime is attained earlier: The imaginary part becomes non-zero at $\gamma = 0.110$ in the achiral case, but at $\gamma < 0.109$ with chirality. The size of the anticrossing, measured vertically between the shifted EP (red-gold junction in Fig. 4c) and the first chiral mode (blue) increases linearly with the chirality of the gap material, with a proportionality coefficient that is close to the value of bulk medium splitting. There is thus a potential for a large sensitivity enhancement.

Coupled-mode theory

The addition of a chiral material in the gap of coupled PT waveguides offers a way for the usually independent TE and TM modes to interact, through interaction of the electric and magnetic fields (see constitutive relations), thereby adding a coupling channel between the two waveguides. To model this interaction, the ‘standard’ PT coupled equations must be supplemented by a coupling between the polarizations. The resulting system can be written in matrix form, in the basis of the isolated waveguide modes, as

$$\frac{i}{k_0}\frac{d}{dz}\begin{pmatrix} TE_g \\ TE_l \\ TM_g \\ TM_l \end{pmatrix} = \begin{pmatrix} n_{TE} - i\gamma_{TE} & C_{TE} & \beta & \alpha \\ C_{TE} & n_{TE} + i\gamma_{TE} & \alpha & \beta \\ \beta^* & \alpha^* & n_{TM} - i\gamma_{TM} & C_{TM} \\ \alpha^* & \beta^* & C_{TM} & n_{TM} + i\gamma_{TM} \end{pmatrix}\begin{pmatrix} TE_g \\ TE_l \\ TM_g \\ TM_l \end{pmatrix}$$

where the subscripts g and l refer to modes of the isolated gain and loss waveguides respectively (see Fig. 1a). $n_{TE/TM}$ and $\gamma_{TE/TM}$ are the effective indices and gain/loss parameters perceived by the isolated modes (without any coupling), and $C_{TE/TM}$ are the coupling constants from conventional directional coupler theory. The last two variables α and β determine the new chiral coupling constants, which are proportional to κ.
The avoided crossings observed in the simulated dispersions are fairly well generated by the eigenvalue dispersion of the coupling matrix (see Fig. 5). For calculations, the achiral parameters $n_{TE/TM}, C_{TE/TM}$ are obtained using the simulated achiral dispersion, while the chiral coupling coefficients α and β are calculated via an overlap integral over the gap area using the simulated achiral supermode profiles at $\gamma = 0$.

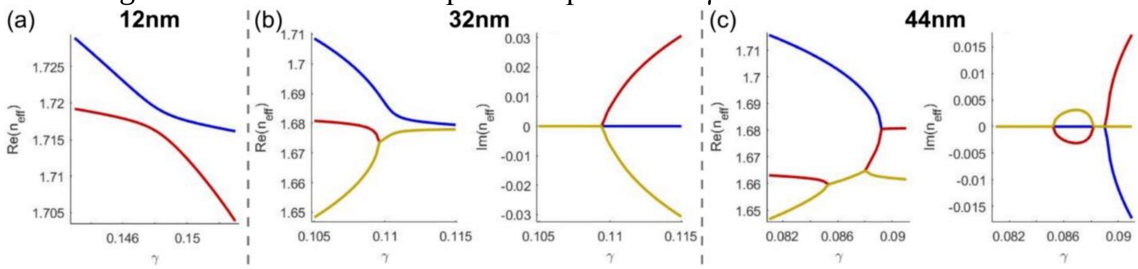

Figure 5 - Eigenvalues of the chiral coupled-mode matrix for the (a) 12 nm, (b) 32 nm, and (c) 44nm gap simulations.

Conclusion

We have shown that the introduction of a chiral material between PT-symmetric waveguides induces avoided crossings in the mode dispersion, of different types depending on the nature of the interacting achiral modes. Furthermore, we have developed a coupled-mode equations model that includes chiral couplings and accurately reproduces the various effects observed in our simulations.

Acknowledgment

This work benefits from the support of the French Community of Belgium within the framework of the financing of a FNRS-FRIA grant.

References

[1] L. Feng, R. El-Ganainy and L. Ge, “Non-Hermitian photonics based on parity-time symmetry,” Nat. Photonics, vol. 11, p. 752, 2017.

[2] M. Hentschel, M. Schaferling, X. Duan, H. Giessen and N. Liu, “Chiral plasmonics,” Sci. Adv., vol. 3, e1602735, 2017.

[3] I. Katsantonis, S. Droulias, C. M. Soukoulis, E. N. Economou, T. P. Rakitzis and M. Kafesaki, “Chirality sensing employing Parity-Time-symmetric and other resonant gain-loss optical systems,” Phys. Rev. B, vol. 105, 2022.

[4] N. Rivolta and B. Maes, “Symmetry recovery for coupled photonic modes with transversal PT symmetry”, Opt. Lett., vol. 40, 2015.